

# Opposing Auxiliary Conformations Produce the Same Torquoselectivity in an Oxazolidinone-Directed Nazarov Cyclization

Bernard L. Flynn,<sup>\*,†</sup> Narasimhulu Manchala,<sup>†</sup> and Elizabeth H. Krenske<sup>\*,‡,§,||</sup>

<sup>†</sup>Medicinal Chemistry, Monash Institute of Pharmaceutical Sciences, Monash University, 381 Royal Parade, Parkville, VIC 3052, Australia

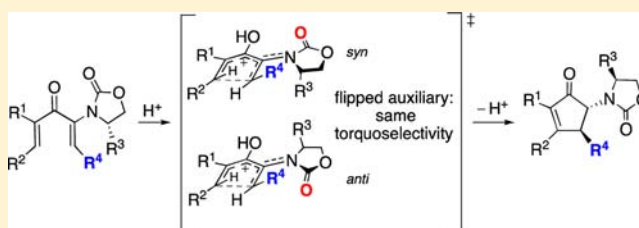
<sup>‡</sup>School of Chemistry and Molecular Biosciences, The University of Queensland, Brisbane, QLD 4072, Australia

<sup>§</sup>School of Chemistry, The University of Melbourne, VIC 3010, Australia

<sup>||</sup>Australian Research Council Centre of Excellence for Free Radical Chemistry and Biotechnology

## S Supporting Information

**ABSTRACT:** Most applications of chiral oxazolidinone auxiliaries in asymmetric synthesis operate through a common set of stereocontrol principles. That is, the oxazolidinone is made to adopt a specific, coplanar conformation with respect to the prochiral substrate, and reaction occurs preferentially at whichever stereoheterotopic face is not blocked by the substituents on the oxazolidinone. In contrast to these principles, we report here the discovery of an alternative mechanism of oxazolidinone-based stereocontrol that does not require coplanarity and is driven instead by allylic strain. This pathway has been uncovered through computational studies of an asymmetric Nazarov cyclization. Chiral oxazolidinone auxiliaries provide essentially complete control over the torquoselectivity of ring closure and the regioselectivity of subsequent deprotonation. Density functional theory calculations (M06-2X//B3LYP) reveal that in the transition state of  $4\pi$  electrocyclic ring closure, the oxazolidinone ring and the cyclizing pentadienyl cation are distorted from coplanarity in a manner that gives two transition state conformations of similar energy. These two conformers are distinguished by a  $180^\circ$  flip in the auxiliary orientation such that in one conformer the oxazolidinone carbonyl is oriented toward the OH of the pentadienyl cation (*syn*-conformer) and in the other it is oriented away from this OH (*anti*-conformer). Surprisingly, both conformations induce the same sense of torquoselectivity, with a 3–5 kcal/mol preference for the *C5- $\beta$*  epimer of the ring-closed cation. In both conformations, the conrotatory mode that leads to the *C5- $\alpha$*  epimer is disfavored due to higher levels of allylic strain between the oxazolidinone substituent and adjacent groups on the pentadienyl cation ( $R^4$  and OH). The excellent torquoselectivities obtained in the oxazolidinone-directed Nazarov cyclization suggest that the allylic strain-driven stereoinduction pathway represents a viable alternative mechanism of stereocontrol for reactions of sterically congested substrates that lie outside of the traditional coplanar (*N*-acyloxazolidinone) paradigm.



## INTRODUCTION

Chiral oxazolidinone auxiliaries provide predictable control over the stereoselectivities of numerous important C–C bond-forming reactions, including enolate alkylation, aldol, Diels–Alder, and radical addition reactions.<sup>1</sup> In all of these applications, stereoinduction is based on a common set of mechanistic features. That is, the oxazolidinone is attached to an unhindered carbonyl group of the substrate, thereby setting up an equilibrium between *syn* and *anti* coplanar conformers (Scheme 1a); addition of a Lewis acid favors one of these conformers, and reaction takes place at the less crowded face (e.g., Scheme 1b). High levels of stereoinduction result from the participation of only one of the possible coplanar conformations (*syn* or *anti*) in the transition state.<sup>2,3</sup>

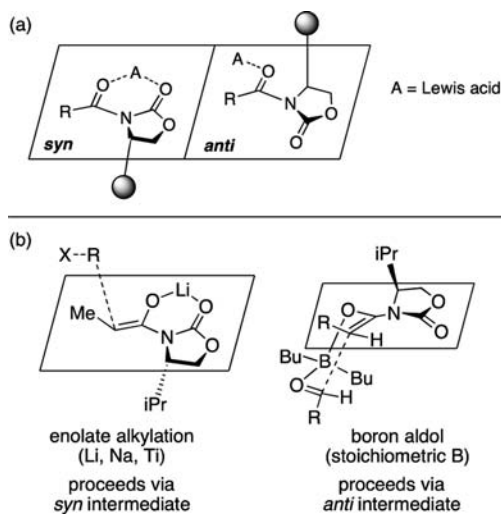
In contrast to these conventional principles, we report here a novel mechanism of oxazolidinone-based stereoinduction that leads to high levels of stereocontrol in reactions of substrates that cannot achieve coplanarity. Recently, we reported<sup>4,5</sup> that

Evans' oxazolidinones act as “master-controllers” of stereo- and regioselectivity in the Nazarov cyclizations<sup>6</sup> of divinyl ketones **1** (Scheme 2), affording a single isomer of the cyclopentenone **4** (*dr* > 20:1). The consistent and essentially complete control over stereo- and regioselectivity in this reaction, together with its applicability to a broad range of substrates (including conventionally resistant substrates), are attractive features for synthetic planning.<sup>7</sup> However, it is not clear how these selectivities arise. We have therefore performed density functional theory calculations to examine the mechanisms of stereo- and regiocontrol. Our calculations, reported here, reveal that a novel and unexpected mechanism of stereoinduction operates in the electrocyclic ring closure of cations **2**. In striking contrast to conventional mechanisms of oxazolidinone-based stereoinduction (Scheme 1), the ring closure of **2** is found to

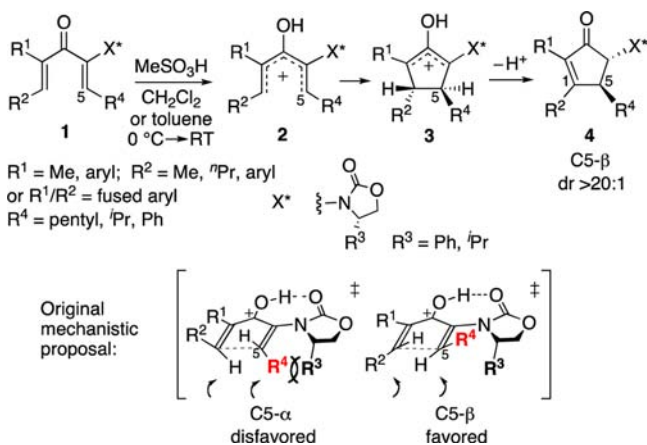
Received: April 11, 2013

Published: June 11, 2013

**Scheme 1.** (a) Syn and Anti Coplanar Conformations of *N*-Oxazolidinyl-Substituted Carbonyl Compounds, and (b) Mechanisms of Stereocontrol in Oxazolidinone-Directed Enolate Alkylation and Aldol Reactions



**Scheme 2.** Oxazolidinone-Directed Asymmetric Nazarov Cyclization<sup>4</sup>



take place through a transition state in which the auxiliary can adopt either a *syn* or an *anti* orientation. In the conventional model of oxazolidinone-based stereoinduction, flipping the auxiliary from the *syn* to the *anti* conformation results in a loss or reversal of induction, but in the Nazarov cyclization the *syn* and *anti* conformers both favor the same stereoisomer of ring-closed product. In this “dual-conformer” scenario, stereoinduction is derived not from differences in facial shielding, but from differences in allylic strain between the pentadienyl cation and the auxiliary in the diastereomeric TSs.

## RESULTS AND DISCUSSION

**Torqueselectivity of Electrocyclization.** Previous computational studies on the Nazarov cyclization have largely dealt with racemic examples, focusing on the effects of substituents on the TS geometries and energies, and exploring the further reactions of the ring-closed cationic intermediate.<sup>8</sup> Chirality transfer in gold-catalyzed and allene variants of the Nazarov cyclization has been studied theoretically by Nieto Faza, de Lera, and co-workers,<sup>8e,h,p,s</sup> while Cavalli, Occhiato, and co-

workers have examined the torqueselectivities of cyclizations involving cyclic vinyl ketones.<sup>8i,l</sup>

To account for the torqueselectivity of ring closure of pentadienyl cations **2**, we previously proposed<sup>4</sup> a transition state model in which a hydrogen bond fixes the oxazolidinone into the *syn* conformation (Scheme 2). In this conformation, the  $\text{R}^3$  group sterically hinders downward rotation by  $\text{R}^4$  but poses no hindrance to upward rotation leading to the C5- $\beta$  product. To investigate this further, we have studied the oxazolidinone-directed ring closure of the model pentadienyl cation **2a** ( $\text{R}^3 = \text{Ph}$ ,  $\text{R}^4 = \text{Me}$ ) by means of density functional theory calculations at the M06-2X/6-311+G(d,p)//B3LYP/6-31G(d) level.<sup>9,10</sup> Geometries were optimized in the gas phase, and SMD<sup>11</sup> single-point calculations were then used to simulate the effects of solvent (dichloromethane or toluene). Figure 1 shows the reactant, transition states, and products of the ring closure of **2a**, together with their computed energies in dichloromethane and in the gas phase.

The calculations predict that the ring closure is irreversible under the experimental conditions ( $\Delta G^\ddagger$  for ring opening = 30 kcal/mol). The torqueselectivity of ring closure is under kinetic control. The experimentally obtained C5- $\beta$  epimer of the ring-closed cation **3a** is 1 kcal/mol less stable than the unobtained C5- $\alpha$  epimer, but the TSs leading to the C5- $\beta$  product (TSC and TSD) are correctly lower in energy than the C5- $\alpha$  TSs. We have termed the two different rotamers of the C5- $\alpha$  and C5- $\beta$  transition states “*syn*” and “*anti*” based on the relationship between the oxazolidinone carbonyl and the protonated divinyl ketone carbonyl (OH), but these two groups lie far from coplanarity. The auxiliary is twisted by 37–49° with respect to the pentadienyl cation. A similar twisted geometry is found in the reactant (**2a**), but the products ( $\alpha$ - and  $\beta$ -**3a**) have essentially achieved coplanarity.

Contrary to our earlier TS model (Scheme 2), the calculations indicate that hydrogen bonding does not take place in the TS leading to the observed product. A hydrogen bond is present in the reactant (**2a-syn**), but not in TSC. The only TS that contains a hydrogen bond is TSA, which is highest in energy and is associated with the unobserved C5- $\alpha$  product. Rotation of the OH group from TSC into a hydrogen-bonded arrangement raised the energy by 3 kcal/mol (see the Supporting Information).

The computed torqueselectivity in dichloromethane (i.e., TSB vs TSD) is large ( $\Delta\Delta G^\ddagger = 3.5$  kcal/mol), in good agreement with the experimental diastereomeric ratios of >20:1 obtained with substituted divinyl ketones.<sup>4</sup> We also fully optimized the transition states TSA–TSD in implicit dichloromethane. Optimization in solvent produced changes of  $\leq 0.5$  kcal/mol in the transition states’ relative energies. As compared to the energies in dichloromethane reported in Figure 1, the predicted torqueselectivity in toluene is smaller (2.0 kcal/mol), but still >20:1.<sup>12,13</sup> Both of these solvents give >20:1 torqueselectivity experimentally.<sup>4</sup>

The lowest-energy transition state for ring closure (TSD) places the oxazolidinone carbonyl *anti* to OH, below the mean plane of the cyclizing group, with the Ph group above the plane. The second C5- $\beta$  TS (TSC) has the oxazolidinone carbonyl *syn* to OH and above the cyclizing moiety, with Ph positioned below. This TS lies 1.4 kcal/mol higher than TSD. Both TSC and TSD are kinetically accessible under the experimental conditions; their computed activation energies correspond to a ratio of about 1:10 at 25 °C. This result is highly unexpected, as it implies that flipping the auxiliary by  $\sim 180^\circ$  has no effect on

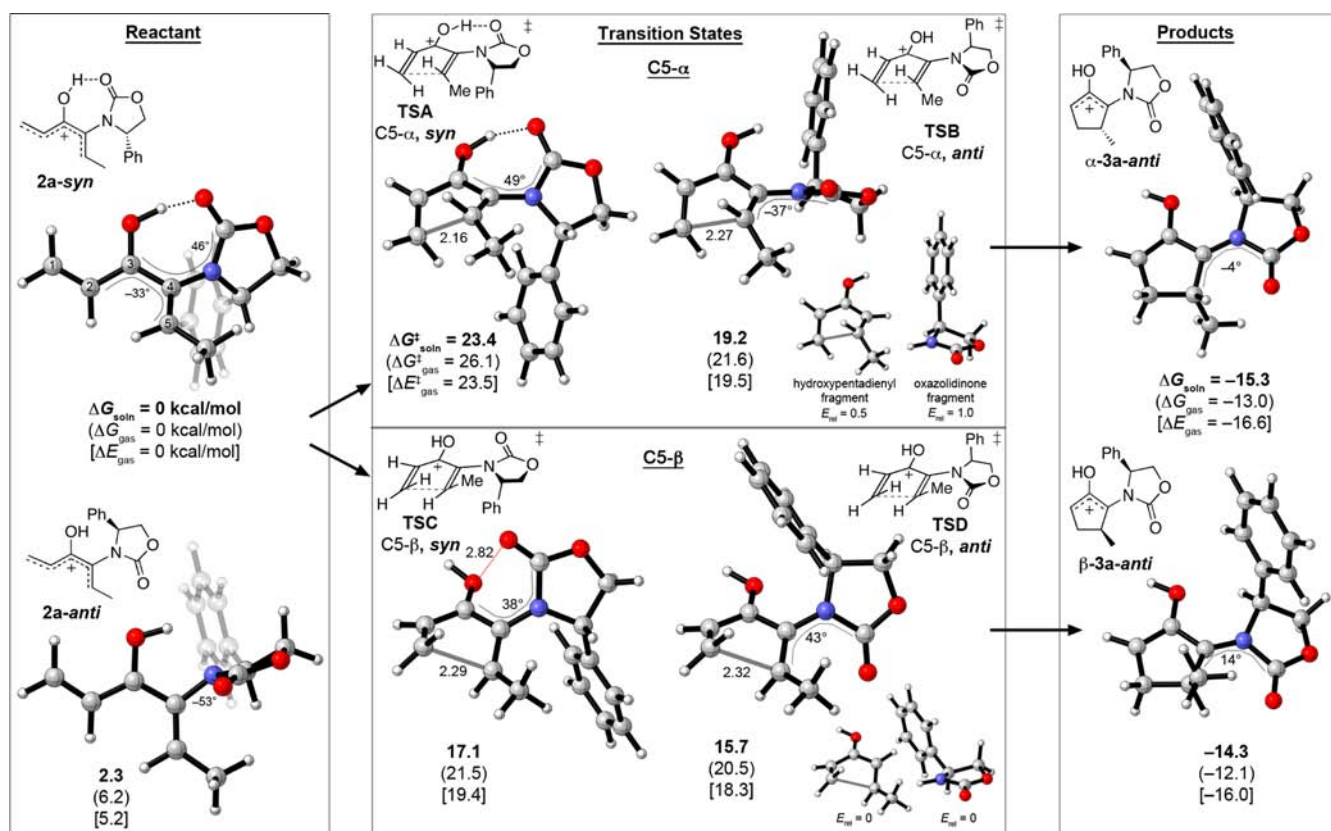


**Figure 1.** The reactant, transition states, and products of electrocyclic ring closure of the oxazolidinone-substituted pentadienyl cation **2a**, computed at the M06-2X/6-311+G(d,p)//B3LYP/6-31G(d) level in conjunction with SMD (M06-2X) solvation corrections. The transition states **TSC** and **TSD** lead to the experimentally obtained stereoisomer of the product. Free energies in dichloromethane are shown in bold, gas-phase free energies are shown in parentheses, and electronic potential energies are shown in brackets (kcal/mol). Distances are given in angstroms. The small insets show the  $\Delta E_{\text{rel}}$  of the pentadienyl and oxazolidinone fragments of **TSB** and **TSD**.

the stereochemical outcome. By contrast, other oxazolidinone-directed reactions invariably rely on the participation of a single, low energy, conformation of the transition state (e.g., Scheme 1), while the presence of multiple low energy conformers, particularly those with reverse orientations of the auxiliary, reduces stereoselectivity.

The torquoselectivity (**TSB** vs **TSD**) can be traced to two factors. There is first a substantial solvent effect. Better solvation of **TSD** (which has a 1.1 D greater dipole moment) contributes 2.4 kcal/mol to the torquoselectivity in dichloromethane. In toluene the solvent effect is 0.9 kcal/mol. The second factor, worth 1.1 kcal/mol, is the degree of allylic strain between the pentadienyl cation and the auxiliary. In the transition state, the oxazolidinone must adopt a conformation that minimizes repulsive interactions with OH and with the upwardly or downwardly rotating  $R^4$  (Me) group. Thus, when the pentadienyl cation termini rotate in the clockwise direction, moving  $R^4$  downward (**TSB**), the oxazolidinone adopts a conformation that places the C=O group upward, away from Me. Conversely, when the conrotation takes place in the anticlockwise direction, moving  $R^4$  upward (**TSD**), the oxazolidinone adopts a conformation that places C=O downward. These two arrangements differ in energy because one (**TSB**) suffers from allylic clashing between Ph and OH. The allylic strain in **TSB** contrasts with the uncluttered arrangement of **TSD** where the Ph group occupies an unhindered region of space above the plane of the cation.

In energy terms, the allylic clashing in **TSB** is manifested as strain within the oxazolidinone. The small insets in Figure 1 depict the pentadienyl and oxazolidinone fragments of transition states **TSB** and **TSD**, and the energies of these isolated fragments,<sup>14</sup> which show that the oxazolidinone is 1 kcal/mol more strained in **TSB** than in **TSD**. The oxazolidinone undergoes distortion in response to the clashing between Ph and OH. The two oxazolidinones also differ with respect to whether the Ph group is pseudoaxial or pseudoequatorial, but the axial/equatorial distinction in itself has negligible energetic consequence.<sup>15</sup> The distortion of the oxazolidinone in response to the allylic clashing in **TSB** is the primary source of torquoselectivity in the gas phase.<sup>16</sup>

In **TSC**, the CHPh group of the oxazolidinone is tilted downward, avoiding a clash with the upwardly rotating Me group. **TSC** is about 1 kcal/mol less stable than **TSD** because of electrostatic repulsion between the oxygen atoms (red line in Figure 1). In **TSA**, the oxazolidinone is unable to avoid severe steric clashing with the Me group. This TS is very high in energy.

**Substituent Effects on Torquoselectivity.** The calculations on **1a**→**3a** reveal an unexpected mechanism of torquoselectivity involving the participation of two different auxiliary conformations. To examine the generality of this mechanism, we computed transition states analogous to **TSA**–**TSD** for a range of other divinyl ketones, **1b**–**g**. The computed activation energies are listed in Table 1.



**Table 1. Predicted Stereoselectivities for Nazarov Cyclizations of Oxazolidinone-Substituted Divinyl Ketones Proceeding through Transition States Analogous to TSA–TSD<sup>a</sup>**

Divinyl ketone	$\Delta G^{\ddagger}_{rel,soln}$ ( $\Delta G^{\ddagger}_{rel,gas}$ )			
	TSA	TSB	TSC	TSD
<b>1a</b> 	7.7 (5.6)	3.5 (1.1)	1.4 (1.0)	0 (0)
<b>1b</b> 	2.2 (-1.3)	3.4 (0.6)	0.5 (-0.4)	0 (0)
<b>1c</b> 	6.4 (3.9)	2.9 (0.4)	1.4 (0.8)	0 (0)
<b>1d</b> 	10.5 (9.4)	3.7 (2.3)	0 (0)	2.6 (3.2)
<b>1e</b> 	6.0 (4.1)	2.9 (0.7)	0 (0)	0.1 (0.2)
<b>1f</b> 	5.6 (4.8)	3.7 (3.9)	0 (-0.3)	0 (0)
<b>1g</b> 	9.2 (8.7)	4.5 (5.2)	0 (0)	2.6 (3.2)

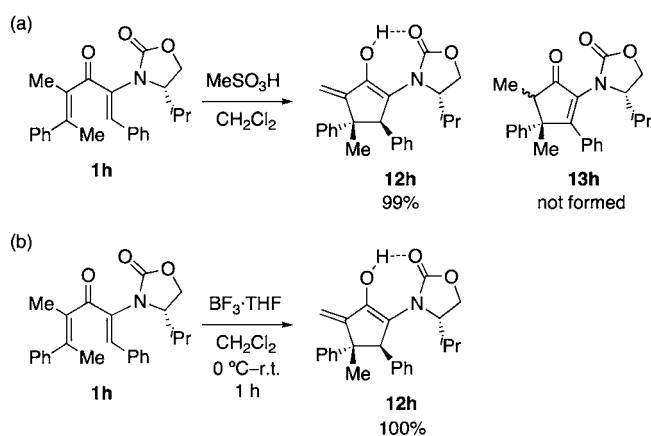
<sup>a</sup>M06-2X-SMD//B3LYP. Relative free energies of activation in dichloromethane are shown (kcal/mol), with gas-phase values in parentheses.

Like **1a**, each of the divinyl ketones **1b–g** is predicted to undergo cyclization favoring the C5- $\beta$  product. The torquoselectivities are slightly higher with the <sup>i</sup>Pr-containing oxazolidinone (**1f,1g**) than with the Ph-containing oxazolidinone (**1a–1e**), and are largest when the divinyl ketone bears a Ph group at R<sup>4</sup> (**1d,1g**), but all are >99:1, consistent with experiment.

The syn/anti conformer preference (TSC vs TSD) depends on the R<sup>4</sup> substituent on the divinyl ketone. A phenyl group at R<sup>4</sup> favors the syn oxazolidinone conformation (TSC, ~80:1). When R<sup>4</sup> is Me or <sup>i</sup>Pr, there is either a slight preference for the anti TS (TSD, ~10:1) or no difference between the syn and anti TS energies. All of the *syn*- $\beta$  transition states favor the non-hydrogen-bonded structure in solution, as seen above for **1a**.

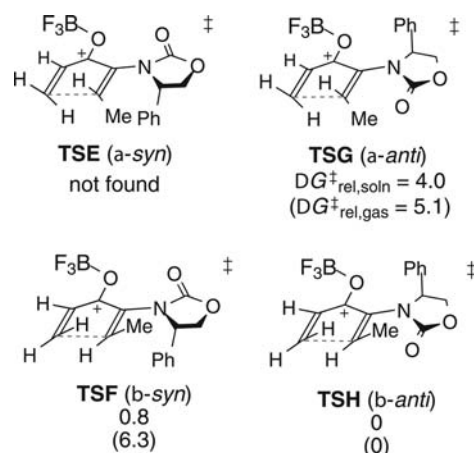
**BF<sub>3</sub> Catalysis of the Nazarov Cyclization.** An experimental test of the theoretically predicted torquoselectivity mechanism was conducted by performing a Nazarov cyclization of **1h** using BF<sub>3</sub> as the catalyst (Scheme 3). The Lewis acid BF<sub>3</sub> rules out any possibility of chelation (which would be analogous to hydrogen bonding) in the syn TS. Previous work<sup>4</sup> had indicated that under Brønsted acid catalysis, the cyclization of **1h** (Scheme 3a) leads exclusively to the C5- $\beta$  enol **12h**. Computed transition states for a model BF<sub>3</sub>-catalyzed

**Scheme 3. (a) Brønsted Acid-Catalyzed<sup>4</sup> and (b) BF<sub>3</sub>-Catalyzed Nazarov Cyclizations of 1h**



cyclization (Scheme 4) predict a large C5- $\beta$  selectivity (4.0 kcal/mol), similar to the Brønsted acid-catalyzed reaction. The

**Scheme 4. Computed Transition States for BF<sub>3</sub>-Catalyzed Electrocyclic Ring Closure of 1a<sup>a</sup>**

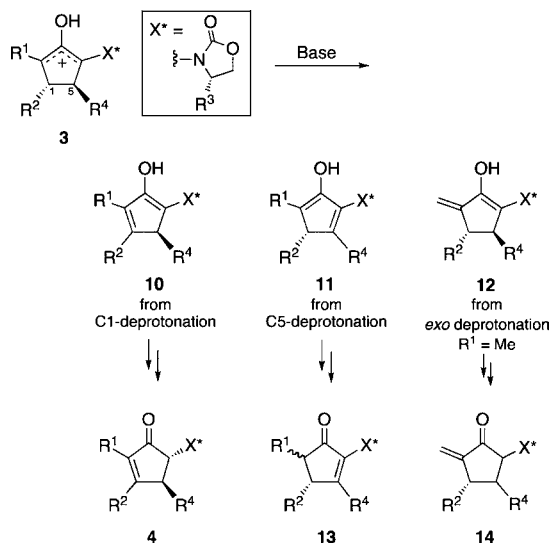


<sup>a</sup>Relative free energies of activation in dichloromethane are shown (M06-2X-SMD//B3LYP, kcal/mol), with gas-phase values in parentheses.

*syn* and anti C5- $\beta$  transition states (TSF and TSH) are close in energy, separated by only 0.8 kcal/mol. Consistent with these predictions, the treatment of **1h** with BF<sub>3</sub>·THF in CH<sub>2</sub>Cl<sub>2</sub> at 0 °C to room temperature (Scheme 3b) was found to lead rapidly and quantitatively to the C5- $\beta$  enol **12h**, the same product as that obtained using the Brønsted acid MeSO<sub>3</sub>H.<sup>4,17</sup>

**Regioselectivity of Cyclopentenone Formation.** Following ring closure, the intermediate **3** undergoes deprotonation and enol–keto tautomerization to give a single regio- and stereoisomer of cyclopentenone **4**. As shown in Scheme 5, the formation of cyclopentenone **4** results from deprotonation of **3** at C1, via enol **10**. None of the isomeric cyclopentenone **13** (derived from deprotonation at C5) is detected. The strict aversion to C5 deprotonation was illustrated synthetically by the Nazarov cyclization of divinyl ketone **1h** (Scheme 3a),<sup>4</sup> where the *exo* double-bonded product **12h** was obtained in essentially quantitative yield. To examine the regioselectivity of cyclopentenone formation, we computed the transition states, intermediates, and products of regioisomeric deprotonation

## Scheme 5. Regioisomeric Pathways for Deprotonation of 3



pathways starting from the ring-closed intermediate  $\beta$ -3c ( $R^1, R^2, R^4 = \text{Me}, R^3 = \text{Ph}$ )<sup>18</sup> using the model base  $\text{NMe}_3$ .<sup>19</sup> Results are shown in Figure 2.

Deprotonation of  $\beta$ -3c at  $R^1$ -Me (TSK) is preferred in the gas phase, but in solution,  $R^1$ -Me and C1 deprotonation (TSI) have about the same energy. Deprotonation at C5 (TSJ) is too high in energy to be significant at experimental temperatures

( $\Delta G_{\text{rel}}^\ddagger = 4.9$  kcal/mol). The C5 deprotonation is disfavored because it requires an unfavorable reorientation of the auxiliary (syn→anti) and because it generates a crowded C=C bond with a methyl group *cis* to an oxazolidinone, as opposed to the less crowded *cis*-dimethyl-substituted C=C bond that is obtained upon C1 deprotonation. Among the three possible enol intermediates **10c**–**12c**, the C1-deprotonated enol **10c** is favored by  $\geq 2.8$  kcal/mol. The corresponding cyclopentenone **4c** is the overall most stable product. Experimentally, cyclization in the presence of catalytic  $\text{MeSO}_3\text{H}$  leads initially to a mixture of *cis*- and *trans*-**4**, but excess acid (10 equiv) accelerates equilibration between these two products to give exclusively the *trans* isomer. The relative activation energies of the TSs and the stabilities of the intermediates in Figure 2 predict that no C5-deprotonation will be detected under the experimental conditions, and any *exo* enol **12** that is formed by  $R^1$ -deprotonation will ultimately be converted back to **3** and then to the thermodynamic product **4**.

## CONCLUSION

Density functional theory calculations reveal that the Nazarov cyclizations of divinyl ketones **1** embody a novel mechanism of oxazolidinone-based stereoreinduction. Theory correctly predicts the torquoselectivities, *cis/trans* diastereoselectivities, and regioselectivities of these reactions. The mechanism of stereoreinduction in the  $4\pi$  electrocyclic ring closure of cations **2** is unexpected, and it represents a striking departure from the well-established mechanisms of stereoreinduction that are known

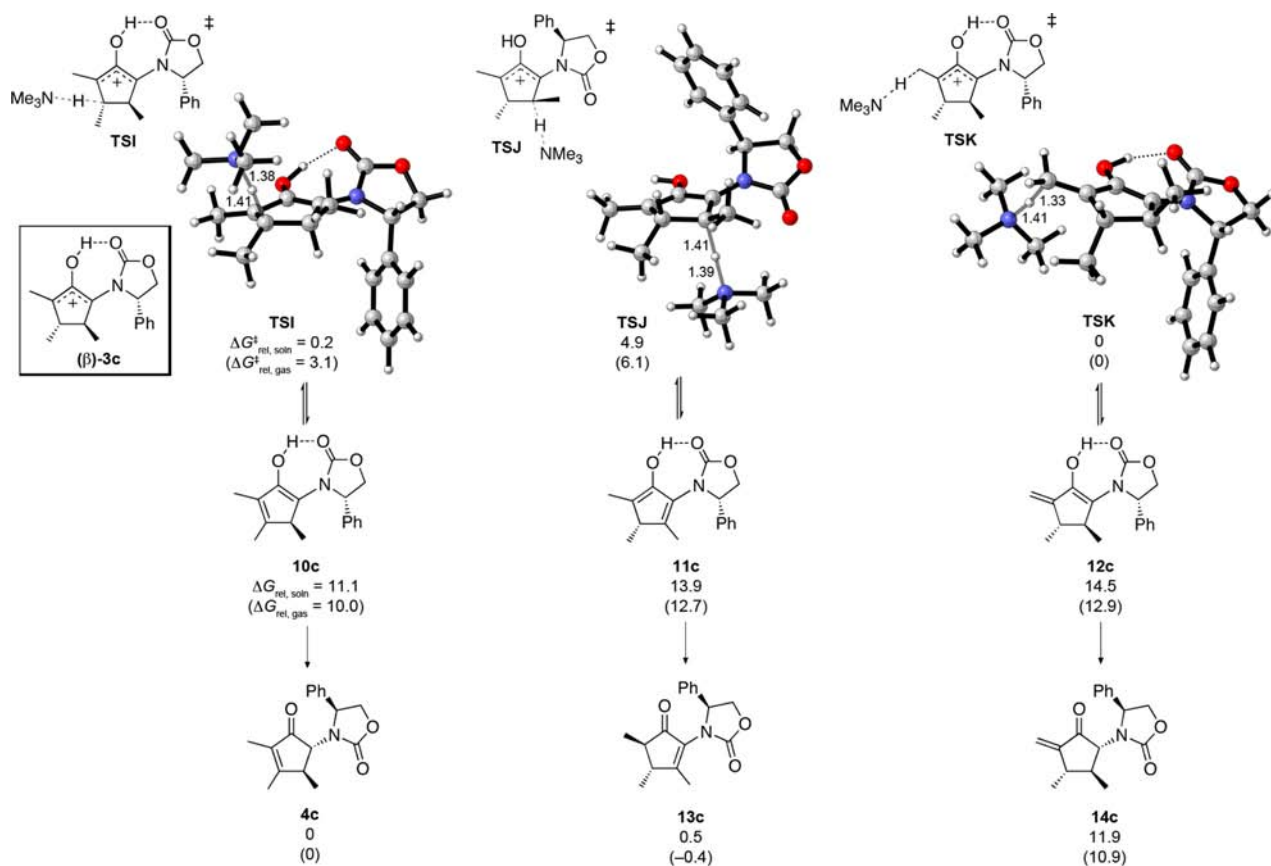
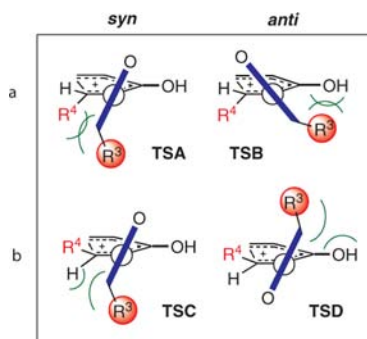


**Figure 2.** Transition states for deprotonation of the ring-closed oxallyl cation ( $\beta$ )-3c by  $\text{NMe}_3$ . TSI leads to the experimentally obtained regioisomer of product, TSJ leads to the other (unobserved) endo regioisomer, and TSK leads to an *exo* methylene group. Relative free energies of isomers in dichloromethane are shown (M06-2X//B3LYP, kcal/mol), with gas-phase values in parentheses.

to apply to most oxazolidinone-directed reactions.<sup>1</sup> In the Nazarov TSs, there is an unusually small energy difference between the syn and anti oxazolidinone orientations. Surprisingly, these two conformations favor the same sense of conrotation, even though opposite faces of the cyclizing cation are shielded in each conformer. The origins of torquoselectivity are summarized pictorially in Scheme 6. Conrotation leading to

**Scheme 6. Pictorial Representation of the Factors Controlling Torquoselectivity in the Nazarov Cyclizations of Oxazolidinone-Substituted Divinyl Ketones 1<sup>a</sup>**



<sup>a</sup>The oxazolidinone is represented by the thick blue line. The transition states are viewed looking down the N–C4 bond.

the  $\alpha$  product is unfavorable with either a syn or an anti oxazolidinone, because both of these TS conformations suffer from steric repulsions between  $R^3$  and the pentadienyl cation substituents ( $R^4$  or OH). Such repulsions are avoided in the  $\beta$  TSs, both syn and anti, because both of these conformations place  $R^3$  well away from groups OH and  $R^4$ .

The usual paradigm of stereoinduction in oxazolidinone-directed asymmetric reactions involves the sole participation of a single, coplanar conformer in the transition state, and stereoinduction results from differences in steric crowding on the two prochiral faces of the substrate. In these situations, flipping the auxiliary by 180° with respect to the prochiral center leads to a loss or reversal of chiral transfer. By contrast, in the “dual-conformer” pathway discovered here for the Nazarov cyclizations of **1**, the two different auxiliary conformations favor the same stereoisomer of product. Stereoinduction does not require coplanarity and is driven by 1,3-allylic strain. While the cyclizing pentadienyl cation adopts a helical transition state in the Nazarov cyclization, it appears unlikely that the allylic-strain driven stereocontrol mechanism is specific to this type of arrangement. What is clear is that high levels of chiral induction can be achieved from noncoplanar intermediates and transition states, which are quite distinct from the types of substrates that are usually considered to be the best venues for oxazolidinone-based stereoinduction (*N*-acyloxazolidinones). High levels of chiral transfer can be achieved through minimization of allylic strain as the new stereocenter ( $sp^2$  to  $sp^3$ ) forms. These principles are likely relevant to various other reactions of sterically congested substrates, where coplanarity between substrate and auxiliary in the TS is likewise not possible. Some notable examples, which have been shown experimentally to afford high levels of stereocontrol, include conjugate additions to  $\alpha$ -substituted *N*-acryloyl oxazolidinones,<sup>20</sup> SmI<sub>2</sub>-promoted cyclizations of *N*-acyloxazolidinones onto alkenes,<sup>21</sup> and tandem  $6\pi$  electrocyclicizations/Diels–Alder cycloadditions of oxazolidinone-sub-

stituted hexatrienes.<sup>22</sup> Allylic strain is also known to influence the stereochemical course of epoxidations and cyclopropanations of oxazolidinone-substituted *cis*-alkenes.<sup>23</sup> Our present findings should be useful for the rationalization of stereoselectivity in these reactions, and for the design of further new methodology for asymmetric synthesis, having revealed that high levels of induction can be achieved through minimization of allylic strain in nonplanar transition states.

## THEORETICAL CALCULATIONS

Density functional theory calculations were performed with the Gaussian 09<sup>24</sup> software. Geometry optimizations and conformational searches were carried out at the B3LYP/6-31G(d) level.<sup>9</sup> Vibrational frequency calculations at this level were used to identify stationary points as minima or transition states and to calculate unscaled thermochemical corrections. Single-point energies were then computed at the M06-2X/6-311+G(d,p) level<sup>10</sup> and used in conjunction with the B3LYP thermochemical corrections to calculate free energies in the gas phase. Free energies in dichloromethane were obtained by addition of SMD<sup>11</sup> solvation energies, computed at the M06-2X/6-31G(d) level. Selected species were also fully optimized in implicit dichloromethane (see the Supporting Information). For comparison with the B3LYP-optimized geometries, the transition states for cyclization of **2a** were also optimized at the M06-2X/6-31G(d) level. The use of M06-2X geometries led to a larger predicted torquoselectivity in dichloromethane ( $\Delta\Delta G^\ddagger = 4.1$  kcal/mol, as compared to 3.5 kcal/mol using B3LYP geometries) and predicted a larger syn/anti energy difference between TSC and TSD ( $\Delta\Delta G^\ddagger = 1.9$  kcal/mol, cf., 1.4 kcal/mol from the B3LYP geometries), but the qualitative conclusions remain the same. A comparison of results obtained with the B3LYP and M06-2X functionals is provided in the Supporting Information. Free energies are reported at 298.15 K at a standard state of 1 mol/L.

## EXPERIMENTAL SECTION

**(S)-3-[(4*R*,5*S*)-2-Hydroxy-4-methyl-3-methylene-4,5-diphenylcyclopent-1-en-1-yl]-4-isopropylloxazolidin-2-one (12h).** BF<sub>3</sub>·THF complex (22  $\mu$ L, 0.2 mmol) was added to a solution of **1h** (111 mg, 0.28 mmol) in CH<sub>2</sub>Cl<sub>2</sub> (2.5 mL) at 0 °C, and the solution was warmed to room temperature over 1 h. After this time, saturated NaHCO<sub>3</sub> aq (7 mL) was added, and the mixture was stirred for 20 min. More CH<sub>2</sub>Cl<sub>2</sub> (10 mL) was added, and the phases were separated. The organic phase was dried over MgSO<sub>4</sub> and concentrated under reduced pressure to afford **12h** (111 mg, 100%), the <sup>1</sup>H NMR spectrum of which was identical to that previously reported.<sup>4</sup>

## ASSOCIATED CONTENT

### Supporting Information

Calculated geometries and energies and a complete citation for ref 24. This material is available free of charge via the Internet at <http://pubs.acs.org>.

## AUTHOR INFORMATION

### Corresponding Author

bernard.flynn@monash.edu; e.krenske@uq.edu.au

### Notes

The authors declare no competing financial interest.

## ACKNOWLEDGMENTS

We acknowledge the financial support of the Australian Research Council Discovery Projects Scheme (DP0985623 to E.H.K. and DP110100835 to B.L.F.) and Future Fellowships Scheme (FT120100632 to E.H.K.) and the ARC Centre of Excellence for Free Radical Chemistry and Biotechnology. Computational resources were provided by the National



Computational Infrastructure National Facility through the National Computational Merit Allocation Scheme (supported by the Australian Government), by the University of Queensland Research Computing Centre, and by the University of Melbourne School of Chemistry. We thank Prof. K. N. Houk for helpful discussions.

## REFERENCES

- (1) (a) Evans, D. A.; Takacs, J. M.; McGee, L. R.; Ennis, M. D.; Mathre, D. J.; Bartroli, J. *Pure Appl. Chem.* **1981**, *53*, 1109–1127. (b) Evans, D. A.; Bartroli, J.; Shih, T. L. *J. Am. Chem. Soc.* **1981**, *103*, 2127–2129. (c) Evans, D. A. *Aldrichimica Acta* **1982**, *15*, 23–32. (d) Evans, D. A.; Chapman, K. T.; Bisaha, J. *J. Am. Chem. Soc.* **1988**, *110*, 1238–1256. (e) Danda, H.; Hansen, M. M.; Heathcock, C. H. *J. Org. Chem.* **1990**, *55*, 173–181. (f) Gothelf, K. V.; Hazell, R. G.; Jørgensen, K. A. *J. Am. Chem. Soc.* **1995**, *117*, 4435–4436. (g) Sibi, M. P.; Ji, J. *Angew. Chem., Int. Ed. Engl.* **1996**, *35*, 190–192. (h) Sibi, M. P.; Ji, J. *J. Am. Chem. Soc.* **1996**, *118*, 3063–3064. (i) Ager, D. J.; Prakash, I.; Schaad, D. R. *Aldrichimica Acta* **1997**, *30*, 3–12. (j) Sibi, M. P.; Ji, J.; Sausker, J. B.; Jasperse, C. P. *J. Am. Chem. Soc.* **1999**, *121*, 7517–7526. (k) Evans, D. A.; Miller, S. J.; Letckta, T.; von Matt, P. *J. Am. Chem. Soc.* **1999**, *121*, 7559–7573. (l) Evans, D. A.; Scheidt, K. A.; Johnston, J. N.; Willis, M. C. *J. Am. Chem. Soc.* **2001**, *123*, 4480–4491. (m) Santos, A. G.; Candeias, S. X.; Afonso, C. A. M.; Jenkins, K.; Caddick, S.; Treweeke, N. R.; Pardoe, D. *Tetrahedron* **2001**, *57*, 6607–6614. (n) Santos, A. G.; Pereira, J.; Afonso, C. A. M.; Frening, G. *Chem.-Eur. J.* **2005**, *11*, 330–343. (o) Evans, D. A.; Helmchen, G.; Rüping, M. In *Asymmetric Synthesis – The Essentials*, 2nd ed.; Christmann, M., Bräse, S., Eds.; Wiley-VCH: Weinheim, 2008; pp 3–9. (p) Lam, Y.-h.; Cheong, P. H.-Y.; Blasco Mata, J. M.; Stanway, S. J.; Gouverneur, V.; Houk, K. N. *J. Am. Chem. Soc.* **2009**, *131*, 1947–1957. (q) Shinisha, C. B.; Sunoj, R. B. *J. Am. Chem. Soc.* **2010**, *132*, 12319–12330. (r) Shinisha, C. B.; Sunoj, R. B. *Org. Lett.* **2010**, *12*, 2868–2871. (s) Rajeev, R.; Sunoj, R. B. *J. Org. Chem.* **2012**, *77*, 2474–2485.
- (2) For alternative explanations of the stereoselectivities of Diels–Alder and conjugate addition reactions of *N*-enoyloxazolidinones, wherein the anti conformer undergoes reaction, see: (a) Bakalova, S. M.; Duarte, F. J. S.; Georgieva, M. K.; Cabrita, E. J.; Santos, A. G. *Chem.-Eur. J.* **2009**, *15*, 7665–7677. (b) Duarte, F. J. S.; Bakalova, S. M.; Cabrita, E. J.; Santos, A. G. *J. Org. Chem.* **2011**, *76*, 6997–7004.
- (3) For selective addition to the more crowded face of an oxazolidinone-substituted oxyallyl intermediate, where contra-steric selectivity is the result of CH– $\pi$  interactions, see: (a) Krenske, E. H.; Houk, K. N.; Lohse, A. G.; Antoline, J. E.; Hsung, R. P. *Chem. Sci.* **2010**, *1*, 387–392. (b) Antoline, J. E.; Krenske, E. H.; Lohse, A. G.; Houk, K. N.; Hsung, R. P. *J. Am. Chem. Soc.* **2011**, *133*, 14443–14451. (c) Du, Y.; Krenske, E. H.; Antoline, J. E.; Lohse, A. G.; Houk, K. N.; Hsung, R. P. *J. Org. Chem.* **2013**, *78*, 1753–1759.
- (4) Kerr, D. J.; Miletic, M.; Chaplin, J. H.; White, J. M.; Flynn, B. L. *Org. Lett.* **2012**, *14*, 1732–1735.
- (5) For earlier approaches to the use of oxazolidinones as chiral auxiliaries in the Nazarov cyclization, see: (a) Pridgen, L. N.; Huang, K.; Shilcrat, S.; Tickner-Eldridge, A.; DeBrosse, C.; Haltiwanger, R. C. *Synlett* **1999**, 1612–1614. (b) Kerr, D. J.; White, J. M.; Flynn, B. L. *J. Org. Chem.* **2010**, *75*, 7073–7084.
- (6) Reviews of the Nazarov cyclization, including asymmetric variants: (a) Denmark, S. E. In *Comprehensive Organic Synthesis*; Trost, B. M., Fleming, I., Paquette, L. A., Eds.; Pergamon: Oxford, 1991; Vol. 5, Chapter 5.6.3, pp 751–784. (b) Habermas, K. L.; Denmark, S. E.; Jones, T. K. *Org. React.* **1994**, *45*, 1–158. (c) Tius, M. A. *Acc. Chem. Res.* **2003**, *36*, 284–290. (d) Harmata, M. *Chemtracts* **2004**, *17*, 416–435. (e) Pellissier, H. *Tetrahedron* **2005**, *61*, 6479–6517. (f) Tius, M. A. *Eur. J. Org. Chem.* **2005**, 2193–2206. (g) Frontier, A. J.; Collison, C. *Tetrahedron* **2005**, *61*, 7577–7606. (h) Grant, T. N.; Rieder, C. J.; West, F. G. *Chem. Commun.* **2009**, 5676–5688. (i) Nakanishi, W.; West, F. G. *Curr. Opin. Drug Discovery Dev.* **2009**, *12*, 732–751. (j) Vaidya, T.; Eisenberg, R.; Frontier, A. J. *ChemCatChem* **2011**, *3*, 1531–1548. (k) Shimada, N.; Stewart, C.; Tius, M. A. *Tetrahedron* **2011**, *67*, 5851–5870. (l) Schotes, C.; Mezzetti, A. *ACS Catal.* **2012**, *2*, 528–538. For a review of mechanistic studies of pentadienyl cation cyclizations, see: (m) Davis, R. L.; Tantillo, D. J. *Curr. Org. Chem.* **2010**, *14*, 1561–1577.
- (7) For other examples of auxiliary-based stereocontrol in the Nazarov cyclization, see: (a) Harrington, P. E.; Tius, M. A. *Org. Lett.* **2000**, *2*, 2447–2450. (b) Harrington, P. E.; Murai, T.; Chu, C.; Tius, M. A. *J. Am. Chem. Soc.* **2002**, *124*, 10091–10100. (c) Kerr, D. J.; Metje, C.; Flynn, B. L. *Chem. Commun.* **2003**, 1380–1381. (d) Dhoro, F.; Kristensen, T. E.; Stockmann, V.; Yap, G. P. A.; Tius, M. A. *J. Am. Chem. Soc.* **2007**, *129*, 7256–7257. (e) Banaag, A. R.; Tius, M. A. *J. Org. Chem.* **2008**, *73*, 8133–8141. (f) Wu, Y.-K.; Niu, T.; West, F. G. *Chem. Commun.* **2012**, 48, 9186–9188 and ref 5.
- (8) For computational studies of Nazarov and related metallaNazarov reactions, see: (a) Smith, D. A.; Ulmer, C. W., II. *Tetrahedron Lett.* **1991**, *32*, 725–728. (b) Smith, D. A.; Ulmer, C. W., II. *J. Org. Chem.* **1991**, *56*, 4444–4447. (c) Smith, D. A.; Ulmer, C. W., II. *J. Org. Chem.* **1993**, *58*, 4118–4121. (d) Smith, D. A.; Ulmer, C. W., II. *J. Org. Chem.* **1997**, *62*, 5110–5115. (e) Iglesias, B.; de Lera, A. R.; Rodríguez-Otero, J.; López, S. *Chem.-Eur. J.* **2000**, *6*, 4021–4033. (f) Nieto Faza, O.; Silva López, C.; Álvarez, R.; de Lera, Á. R. *Chem.-Eur. J.* **2004**, *10*, 4324–4333. (g) Harmata, M.; Schreiner, P. R.; Lee, D. R.; Kirchofer, P. L. *J. Am. Chem. Soc.* **2004**, *126*, 10954–10957. (h) Nieto Faza, O.; Silva López, C.; Álvarez, R.; de Lera, Á. R. *Chem. Commun.* **2005**, 4285–4287. (i) Cavalli, A.; Masetti, M.; Recanatini, M.; Prandi, C.; Guarna, A.; Occhiato, E. G. *Chem.-Eur. J.* **2006**, *12*, 2836–2845. (j) Shi, F.-Q.; Li, X.; Xia, Y.; Zhang, L.; Yu, Z.-X. *J. Am. Chem. Soc.* **2007**, *129*, 15503–15512. (k) Lemièrre, G.; Gandon, V.; Cariou, K.; Fukuyama, T.; Dhimane, A.-L.; Fensterbank, L.; Malacria, M. *Org. Lett.* **2007**, *9*, 2207–2209. (l) Cavalli, A.; Pacetti, A.; Recanatini, M.; Prandi, C.; Scarpi, D.; Occhiato, E. G. *Chem.-Eur. J.* **2008**, *14*, 9292–9304. (m) Marcus, A. P.; Lee, A. S.; Davis, R. L.; Tantillo, D. J.; Sarpong, R. *Angew. Chem., Int. Ed.* **2008**, *47*, 6379–6383. (n) Cordier, P.; Aubert, C.; Malacria, M.; Lacôte, E.; Gandon, V. *Angew. Chem., Int. Ed.* **2009**, *48*, 8757–8760. (o) Lemièrre, G.; Gandon, V.; Cariou, K.; Hours, A.; Fukuyama, T.; Dhimane, A.-L.; Fensterbank, L.; Malacria, M. *J. Am. Chem. Soc.* **2009**, *131*, 2993–3006. (p) Nieto Faza, O.; Silva López, C.; de Lera, A. R. *J. Org. Chem.* **2011**, *76*, 3791–3796. (q) Krafft, M. E.; Vidhani, D. V.; Cran, J. W.; Manoharan, M. *Chem. Commun.* **2011**, 47, 6707–6709. (r) Lebœuf, D.; Huang, J.; Gandon, V.; Frontier, A. J. *Angew. Chem., Int. Ed.* **2011**, *50*, 10981–10985. (s) González-Pérez, A. B.; Vaz, B.; Nieto Faza, O.; de Lera, Á. R. *J. Org. Chem.* **2012**, *77*, 8733–8743. (t) Lebœuf, D.; Gandon, V.; Ciesielski, J.; Frontier, A. J. *J. Am. Chem. Soc.* **2012**, *134*, 6296–6308. (u) Lebœuf, D.; Theiste, E.; Gandon, V.; Daifuku, S. L.; Neidig, M. L.; Frontier, A. J. *Chem.-Eur. J.* **2013**, *19*, 4842–4848.
- (9) (a) Lee, C.; Yang, W.; Parr, R. G. *Phys. Rev. B* **1988**, *37*, 785–789. (b) Becke, A. D. *J. Chem. Phys.* **1993**, *98*, 1372–1377. (c) Becke, A. D. *J. Chem. Phys.* **1993**, *98*, 5648–5652. (d) Stephens, P. J.; Devlin, F. J.; Chabalowski, C. F.; Frisch, M. J. *J. Phys. Chem.* **1994**, *98*, 11623–11627.
- (10) (a) Zhao, Y.; Truhlar, D. G. *Theor. Chem. Acc.* **2008**, *120*, 215–241. (b) Zhao, Y.; Truhlar, D. G. *Acc. Chem. Res.* **2008**, *41*, 157–167.
- (11) Marenich, A. V.; Cramer, C. J.; Truhlar, D. G. *J. Phys. Chem. B* **2009**, *113*, 6378–6396.
- (12) For comparison with the SMD values, we also computed solvent effects with another continuum model (CPCM<sup>13</sup>). The relative energies of TSA–TSD in CPCM dichloromethane varied by 0–0.4 kcal/mol from the corresponding SMD values.
- (13) (a) Barone, V.; Cossi, M. *J. Phys. Chem. A* **1998**, *102*, 1995–2001. (b) Cossi, M.; Rega, N.; Scalmani, G.; Barone, V. *J. Comput. Chem.* **2003**, *24*, 669–681.
- (14) The energy difference between the pseudoaxial and pseudoequatorial oxazolidinones in TSB and TSD was determined by replacing the pentadienyl moiety by an H atom ( $r_{\text{NH}} = 1.09 \text{ \AA}$ ) while leaving the remaining atoms fixed. Single-point energies ( $E$ ) of the truncated structures were computed at the M06-2X/6-311+G(d,p) level.

(15) Fully optimized pseudoaxial and pseudoequatorial oxazolidinones differ by only 0.1 kcal/mol.

(16) Between the pentadienyl cation fragments of **TSB** and **TSD**, there is a small (0.5 kcal/mol) energy difference favoring **TSD**, which reflects the less advanced bond formation in **TSD**. The orientation of the oxazolidinone in **TSB** actually leads to a stabilizing OH $\cdots\pi$  interaction between OH and Ph. However, this interaction does not offset the distortions of the oxazolidinone and pentadienyl cation.

(17) West et al. (ref 7f) recently reported Nazarov cyclizations of oxazolidinonyl-substituted divinyl ketones promoted by superstoichiometric quantities (5 equiv) of triflic acid, and proposed the intermediacy of superelectrophilic diprotonated or protosolvated intermediates. We explored computationally the possibility of double protonation (one H<sup>+</sup> on each carbonyl); these calculations predicted C5- $\beta$  selectivity. However, although the most usual experimental protocol in our laboratory (ref 4) involved the use of 3–10 equiv of MeSO<sub>3</sub>H, the excess acid was simply added to accelerate conversion of the initial mixture of C4–C5 cis/trans isomers of **4** into the thermodynamic product, the trans isomer. The same torquoselectivities were obtained with catalytic MeSO<sub>3</sub>H (3–5 mol%).

(18) Unlike ( $\beta$ )-**3a**, the most stable isomer of ( $\beta$ )-**3c** has the syn conformation.

(19) Under the experimental conditions, the actual base is likely to be the methanesulfonate counterion, the solvent, or another molecule of substrate/product.

(20) Wu, M.-J.; Yeh, J.-Y. *Tetrahedron* **1994**, *50*, 1073–1082.

(21) Taaning, R. H.; Thim, L.; Karaffa, J.; Campaña, A. G.; Hansen, A.-M.; Skrydstrup, T. *Tetrahedron* **2008**, *64*, 11884–11895.

(22) (a) Hayashi, R.; Feltenberger, J. B.; Hsung, R. P. *Org. Lett.* **2010**, *12*, 1152–1155. (b) Hayashi, R.; Walton, M. C.; Hsung, R. P.; Schwab, J. H.; Yu, X. *Org. Lett.* **2010**, *12*, 5768–5771. (c) Hayashi, R.; Ma, Z.-X.; Hsung, R. P. *Org. Lett.* **2012**, *14*, 252–255.

(23) (a) Adam, W.; Bosio, S. G.; Wolff, B. T. *Org. Lett.* **2003**, *5*, 819–822. (b) Song, Z.; Lu, T.; Hsung, R. P.; Al-Rashid, Z. F.; Ko, C.; Tang, Y. *Angew. Chem., Int. Ed.* **2007**, *46*, 4069–4072. See also: (c) Sivaguru, J.; Saito, H.; Poon, T.; Omonuwa, T.; Franz, R.; Jockusch, S.; Hooper, C.; Inoue, Y.; Adam, W.; Turro, N. J. *Org. Lett.* **2005**, *7*, 2089–2092.

(24) Frisch, M. J.; et al. *Gaussian 09*, revision C.01; Gaussian, Inc.: Wallingford, CT, 2010.